Theory of nondegenerate four-wave mixing between pulses in a semiconductor waveguide

Mørk, Jesper; Mecozzi, A.

Published in:
I E E E Journal of Quantum Electronics

Link to article, DOI:
10.1109/3.563382

Publication date:
1997

Document Version
Publisher's PDF, also known as Version of record

Theory of Nondegenerate Four-Wave Mixing Between Pulses in a Semiconductor Waveguide

J. Mørk and A. Mecozzi

***Abstract*—We develop a perturbation theory for calculating the effects of saturation on nondegenerate four-wave mixing between short optical pulses in a semiconductor optical amplifier. Saturation due to ultrafast intraband dynamics like carrier heating and spectral hole burning is found to be important for pulses on the order of 10–20 ps or less.**

***Index Terms*— Optical mixing, optical pulses, semiconductor waveguides.**

I. Introduction

THE phenomenon of nondegenerate four-wave mixing (FWM) in semiconductor optical amplifiers has several important applications in high-capacity optical communication systems. Dispersion compensation using midspan spectral inversion [1], wavelength conversion [2], [3], and demultiplexing of high-bit-rate time-division multiplexed pulse trains [4] are important examples of all-optical signal processing techniques based on FWM, which have been experimentally demonstrated to have a significant potential in future broadband optical networks. In addition, FWM has shown to be a useful spectroscopic technique for investigating the physical origin of ultrafast nonlinearities in active semiconductor waveguides [5]–[8].

Several papers [9]–[14] have already been devoted to the theoretical analysis of FWM in semiconductor optical amplifiers. Good agreement between experiment and theory has been demonstrated in the case of FWM among CW beams, both in terms of the detuning dependence [7], [8] and the saturation behavior [15]. In contrast, much less work has been carried out for the case of FWM among short pulses [16], which is the most important case for practical applications. An important exception is the paper by Shtaif and Eisenstein [17], calculating the FWM efficiency and saturation characteristics for optical pulses. Those calculations are, however, limited to pulsewidths of the order of 10–20 ps or longer, because they neglect the contribution of the ultrafast dynamics on the gain saturation. In this paper, we present analytical calculations of the FWM efficiency based on a response function approach [18]–[20] and demonstrate the important influence of the ultrafast gain dynamic processes for the saturation behavior.

The calculations are based on a perturbative treatment for the induced gain and index changes as well as for the field propagation. Including only first-order terms yields results which do not include nonlinear saturation effects. Such a theory is directly applicable to the analysis of spectroscopic measurements, which are commonly carried out in the linear regime.

To evaluate the influence of saturation effects, a second-order perturbation theory should be used. The material dynamics are still treated as being linear, but the effect of saturation on the propagation of the fields is then taken into account. By this, the effects of carrier density changes, carrier heating, and spectral hole burning (SHB) are treated on equal footing. This is reasonable for a single pair of short pulses, since gain saturation calculations [21] show these effects to be comparable for pulses shorter than 10–20 ps. The effects of coupling between the different saturation mechanisms for the material susceptibility itself is not included. The coupling of the carrier heating and SHB contributions with the saturation of the carrier density was shown to be important in the CW case, [15] but in the present short-pulse low-repetition case, second-order effects in the carrier heating and SHB mechanisms themselves are expected to be equally important.

Strictly speaking, this paper is limited to the analysis of a single pair of optical pulses interacting in the semiconductor medium. In many practical applications, however, the situation will be that of a train of short optical (signal or probe) pulses at a high repetition rate interacting with another train of stronger (sampling or pump) pulses, at a relatively low repetition rate. In this case, the saturation effect of the signal beam may be treated on an average power basis to provide an effective gain, while the analysis of the present paper can be invoked to understand the saturation effects of the sampling beam. Our conclusions, therefore, also pertain to this important practical example.

The paper is organized as follows: in Section II, we present the basic equations for treating pulse propagation and material dynamics and make a general perturbation analysis. Specific expressions for the FWM efficiency are derived in the linear regime of first-order perturbation theory, Section II-A, and in the saturation regime, Section II-B, where the analysis is taken to second-order. The results are illustrated and discussed in Section III, and finally our conclusions are summarized in Section IV.

II. Propagation Equations

Given the real electric field $\mathcal{E}(z,t)$, the slowly varying envelope $E(z,t)$ is defined as

$$\mathcal{E}(z,t) = E(z,t)e^{-i\omega_0 t + ik_0 z} + c.c. \tag{1}$$

where ω_0 is the reference optical frequency and $k_0 = \omega_0 n_0/c$ is the wavenumber determined by the background refractive

Manuscript received June 10, 1996; revised December 9, 1996.

J. Mørk is with Mikroelektronik Centret, Technical University of Denmark, DK-2800 Lyngby, Denmark. He was with Tele Danmark R&D, Lyngsø Allé 2, DK-2970 Hørsholm, Denmark.

A. Mecozzi is with Fondazione Ugo Bordoni, 00142, Rome, Italy.

Publisher Item Identifier S 0018-9197(97)02344-0.

index $n_0 = n(\omega_0)$. In [19], the following propagation equation is derived for the slowly varying envelope field $E(z,t)$:

$$\frac{\partial E(z,t)}{\partial z} = \mathcal{L}(t)E(z,t) + R(z,t) \tag{2}$$

with the linear operator $\mathcal{L}$ defined by

$$\mathcal{L}(t) = \frac{1}{2}\xi\left(\omega_0 + i\frac{\partial}{\partial t}\right) + i\kappa\left(\omega_0 + i\frac{\partial}{\partial t}\right) \tag{3}$$

where $\kappa = k(\omega) - k(\omega_0)$ is the wavenumber change from the reference value k_0, and

$$\xi = \Gamma g - \alpha_{\text{int}} \tag{4}$$

is the net modal gain, with Γ being the confinement factor, g the material gain, and α_{int} the internal loss. The source term $R(z,t)$ is given by

$$R(z,t) = \int_{-\infty}^{\infty} h(t-t')|E(z,t')|^2 dt' E(z,t) \tag{5}$$

where $h(t)$ is the response function of the medium (see Appendix A), calculated using the adiabatic approximation for the dynamics of the medium polarization [18].

We emphasize here that the local gain and index changes induced by the field are approximated as being linear in the local intensity, cf. (5). In reality, carrier density changes, e.g., induced by the field, saturates with increasing intensity due to the "back-action" of the induced gain change and leads to correction terms of order $|E|^4E$ in the propagation equation (2). The same holds true for the contributions from SHB and carrier heating and even leads to a mutual interdependence of the different contributions (see also [15]). We are treating here the case of very short pulses, where the contributions from the ultrafast processes and the carrier density changes are comparable and therefore have to be treated within the same approximation. The neglect of the higher order terms in (2) means that only *saturation* effects to second-order in the field should be analyzed on the basis of that equation.

We shall treat the source term $R(z,t)$ as a perturbation and calculate the changes it induces to the electric field propagating in the waveguide to second-order in the perturbation. Thus, expanding the field as

$$E(z,t) = E^{(0)}(z,t) + E^{(1)}(z,t) + E^{(2)}(z,t) \tag{6}$$

we get the following hierarchy of equations:

$$\frac{\partial E^{(0)}(z,t)}{\partial z} = \mathcal{L}(t)E^{(0)}(z,t) \tag{7}$$

$$\frac{\partial E^{(n)}(z,t)}{\partial z} = \mathcal{L}(t)E^{(n)}(z,t) + R^{(n-1)}(z,t), \quad n = 1,2 \tag{8}$$

with

$$R^{(0)}(z,t) = \int_{-\infty}^{\infty} h(t-t')|E^{(0)}(z,t')|^2 dt' E^{(0)}(z,t) \tag{9}$$

$$\begin{aligned} R^{(1)}(z,t) = &\int_{-\infty}^{\infty} h(t-t')|E^{(0)}(z,t')|^2 dt' E^{(1)}(z,t) \\ &+ \int_{-\infty}^{\infty} h(t-t')[E^{(0)}(z,t')E^{(1)*}(z,t') \\ &+ E^{(0)*}(z,t')E^{(1)}(z,t')]E^{(0)}(z,t). \end{aligned} \tag{10}$$

The solution of (7) with initial condition $E^{(0)}(0,t) = E(0,t)$ is

$$E^{(0)}(z,t) = \exp\{z\mathcal{L}(t)\}E(0,t) \tag{11}$$

and the solution of (8) with initial conditions $E^{(n)}(0,t) = 0$, $n = 1,2$, is

$$E^{(n)}(z,t) = \int_0^z dz' \exp\{(z-z')\mathcal{L}(t)\}R^{(n-1)}(z',t). \tag{12}$$

In [19], the first-order result was used to analyze frequency-degenerate pump-probe measurements employing ultrashort optical pulses. Here, we shall apply the formalism to the case of nondegenerate four-wave mixing. The first-order result already includes the generation of a conjugate signal, but by taking the calculation to second-order we can also study the effects of saturation on the generation of the conjugate signal.

We now decompose the total electric field into components corresponding to the pump frequency ω_0, the probe frequency ω_1, and the conjugate frequency $\omega_2 = \omega_0 - (\omega_1 - \omega_0)$:

$$\begin{aligned} E(z,t) &= E_0(z,t) + E_1(z,t) + E_2(z,t) \\ &= A_0(z,t) + A_1(z,t)\mathrm{e}^{-i\Omega_1 t} + A_2(z,t)\mathrm{e}^{-i\Omega_2 t} \end{aligned} \tag{13}$$

with

$$\Omega_1 = \omega_1 - \omega_0; \quad \Omega_2 = \omega_2 - \omega_0 = -\Omega_1. \tag{14}$$

With these definitions, the spectra of the envelope fields A_j are centered at DC. Applying the decomposition (13) also for the different orders in the perturbation expansion, inserting into (10)–(12), and separating terms at DC, $e^{-i\Omega_1 t}$ and $e^{-i\Omega_2 t}$ we can then obtain expressions for the pump, probe and conjugate fields. In this most general form, the theory can be used to analyze the influence on the conjugate signal of dispersion, leading to pulse broadening and phase mismatch, as well as chirp.

Here, we shall limit ourselves to linear index dispersion. The neglect of group velocity dispersion is a good approximation for pulses longer than 100 fs [22] and frequency detunings $|\Omega_1|/2\pi$ less than 10 THz [12]. We then have

$$\mathcal{L}(t) \simeq \frac{1}{2}\xi\left(\omega_0 + i\frac{\partial}{\partial t}\right) - \kappa'\frac{\partial}{\partial t} \tag{15}$$

where $\kappa' = 1/v_g$, with v_g being the group velocity. The last term of (15) can be removed by transforming to a frame moving with the group velocity, i.e., we introduce local time t by $t \to t + \kappa' z$. Henceforth, t denotes local time.

Rather than utilizing the approximated $\mathcal{L}$ directly in (10)–(12), we shall take the approach of first formulating propagation equations for the pump, probe, and conjugate envelope fields. In the action of the operator $\mathcal{L}$ on the electrical field, we shall assume the envelope to be slowly varying in comparison with $e^{-i\Omega_{1,2}t}$. This approximation is consistent with the inherent assumption that the spectra of pump, probe, and conjugate can be separated and leads to

$$\mathcal{L}(t)E_j(z,t) \simeq L_j E_j(z,t) \tag{16}$$

with the constants L_j defined as

$$L_j = \frac{1}{2}\xi(\omega_j) = \frac{1}{2}\xi_j, \quad j = 0,1,2. \tag{17}$$

Inserting the decomposition (13) into (2) and (5), assuming the pump to be much stronger than the probe and conjugate fields

$$|A_0|^2 \gg |A_1|^2, |A_2|^2 \tag{18}$$

and separating the field components, we get the following set of propagation equations:

$$\frac{\partial A_j(z,t)}{\partial z} = L_j A_j(z,t) + R_j(z,t) \tag{19}$$

with the source terms defined as

$$R_0(z,t) = \int_{-\infty}^{\infty} h(t')|A_0(z,t-t')|^2 dt' A_0(z,t) \tag{20}$$

$$\begin{aligned} R_1(z,t) = &\int_{-\infty}^{\infty} h(t')|A_0(z,t-t')|^2 dt' A_1(z,t) \\ &+ \int_{-\infty}^{\infty} h(t') A_0^*(z,t-t') A_1(z,t-t') \\ &\times e^{i\Omega_1 t'} dt' A_0(z,t) \\ &+ \int_{-\infty}^{\infty} h(t') A_0(z,t-t') A_2^*(z,t-t') \\ &\times e^{i\Omega_1 t'} dt' A_0(z,t) \end{aligned} \tag{21}$$

$$\begin{aligned} R_2(z,t) = &\int_{-\infty}^{\infty} h(t')|A_0(z,t-t')|^2 dt' A_2(z,t) \\ &+ \int_{-\infty}^{\infty} h(t') A_0^*(z,t-t') A_2(z,t-t') \\ &\times e^{i\Omega_2 t'} dt' A_0(z,t) \\ &+ \int_{-\infty}^{\infty} h(t') A_0(z,t-t') A_1^*(z,t-t') \\ &\times e^{i\Omega_2 t'} dt' A_0(z,t). \end{aligned} \tag{22}$$

In the integrals over t', we made the transformation $t' \to t - t'$. The condition for separating the frequency components is of course that the spectral widths of the pump and probe pulses are much smaller than the frequency separation, i.e.,

$$\frac{1}{\tau_{p0}}, \frac{1}{\tau_{p1}} \ll |\Delta\Omega_1| \tag{23}$$

where τ_{p0} and τ_{p1} are the temporal widths of pump and probe pulses. In (20)–(22), the terms containing $|A_0|^2$ reflect saturation due to the pump. The terms containing $A_0 A_j^*$ (or $A_0^* A_j$), $j = 1, 2$, reflect mixing between the pump at ω_0 and the signal at ω_j, which leads to a temporal "grating" that scatters the pump to the frequency ω_{3-j} (or ω_j).

Applying the perturbation expansion

$$A(z,t) = A^{(0)}(z,t) + A^{(1)}(z,t) + A^{(2)}(z,t) \tag{24}$$

we get for the different orders

$$\frac{\partial A_j^{(0)}(z,t)}{\partial z} = L_j A_j^{(0)}(z,t) \tag{25}$$

$$\frac{\partial A_j^{(n)}(z,t)}{\partial z} = L_j A_j^{(n)}(z,t) + R_j^{(n-1)}(z,t), \quad n = 1, 2. \tag{26}$$

With initial conditions

$$A_j^{(0)}(0,t) = A_j(0,t); \quad A_j^{(n)}(0,t) = 0, \quad n = 1, 2 \tag{27}$$

the solutions are

$$A_j^{(0)}(z,t) = \exp[zL_j] A_j(0,t), \tag{28}$$

$$A_j^{(n)}(z,t) = \int_0^z dz' \exp[(z-z')L_j(t)] R_j^{(n-1)}(z',t), \quad n = 1, 2. \tag{29}$$

The expressions for the source terms $R_j^{(0)}$ and $R_j^{(1)}$ follow from (20) to (22) by collecting terms of zeroth- and first-order, respectively, and will be given in the following two sections.

A. Linear Regime—First-Order Perturbation Theory

We shall limit ourselves to the usual case where, at the input of the waveguide, signals are injected only at the pump and the probe frequency, i.e.,

$$A_2(0,t) = 0. \tag{30}$$

Using (28), we then get

$$R_0^{(0)}(z,t) = e^{3L_0 z} \int_{-\infty}^{\infty} h(t')|A_0(0,t-t')|^2 dt' A_0(0,t) \tag{31}$$

$$\begin{aligned} R_1^{(0)}(z,t) = &e^{2L_0 z + L_1 z} \int_{-\infty}^{\infty} h(t')|A_0(0,t-t')|^2 dt' A_1(0,t) \\ &+ e^{2L_0 z + L_1 z} \int_{-\infty}^{\infty} h(t') A_0^*(0,t-t') A_1(0,t-t') \\ &\times e^{i\Omega_1 t'} dt' A_0(0,t) \end{aligned} \tag{32}$$

$$\begin{aligned} R_2^{(0)}(z,t) = &e^{2L_0 z + L_1 z} \int_{-\infty}^{\infty} h(t') A_0(0,t-t') A_1^*(0,t-t') \\ &\times e^{i\Omega_2 t'} dt' A_0(0,t). \end{aligned} \tag{33}$$

The wave mixing terms in (31)–(33) are governed by expressions of the form

$$F_{ij}(\Omega,t) = \int_{-\infty}^{\infty} h(t') A_i^*(0,t-t') A_j(0,t-t') e^{i\Omega t'} dt'. \tag{34}$$

Defining the Fourier transform pair

$$y(\Omega) = \int_{-\infty}^{\infty} y(t) e^{i\Omega t} dt \tag{35}$$

$$y(t) = \int_{-\infty}^{\infty} y(\Omega) e^{-i\Omega t} \frac{d\Omega}{2\pi} \tag{36}$$

we have

$$\begin{aligned} F_{ij}(\Omega,t) &= \int_{-\infty}^{\infty} h(\Omega - \Omega') I(\Omega', t) \frac{d\Omega'}{2\pi} \\ &= h(\Omega) \otimes I_{ij}(\Omega, t) \end{aligned} \tag{37}$$

with

$$I_{ij}(t',t) = A_i^*(0,t-t') A_j(0,t-t') \tag{38}$$

so that

$$\begin{aligned} I_{ij}(\Omega,t) &= \int_{-\infty}^{\infty} A_i^*(0,t-t') A_j(0,t-t') e^{i\Omega t'} dt' \\ &= A_i(0,\Omega)^* \otimes A_j(0,-\Omega) e^{i\Omega t}. \end{aligned} \tag{39}$$

This expression shows that the spectrum $I_{ij}(\Omega,t)$ is centered around $\Omega=0$ and has a width given by the width of the convolved spectra of A_i and A_j. Now, the wave mixing terms in (31)–(33) are governed by $F_{ij}(\Omega=\Omega_{1,2},t)$. Let us assume that in addition to the relation (23) the spectrum of the response function, $h(\Omega)$, varies slowly over an interval around $\Omega=\Omega_{1,2}$, given by the spectral width of $I_{ij}(\Omega,t)$. Then

$$F_{ij}(\Omega,t)\simeq h(\Omega)\int_{-\infty}^{\infty}I_{ij}(\Omega',t)\frac{d\Omega'}{2\pi}$$
$$=h(\Omega)A_i^*(0,t)A_j(0,t),\quad \Omega=\Omega_1,\Omega_2. \tag{40}$$

This approximation can also be inferred by noting, from the definition of F_{ij}, that for frequencies Ω for which the separation is possible, the exponential factor $e^{i\Omega t'}$ varies quickly compared to the field amplitudes, which can be taken outside of the integral with $t'=0$, since the response function peaks here.

The terms in (31)–(33) expressing saturation by the pump are governed by $F_{00}(\Omega=0,t)$. The appropriate approximation for this quantity depends on the relaxation time constants of $h(t)$. Let us write h on the form

$$h(t)=h_s(t)+h_f(t) \tag{41}$$

where $h_s(t)$ are the components of h whose exponential decay time is slow compared with the width of the pump pulse and h are the components which are fast. Then

$$F_{00}(\Omega=0,t)=\int_{-\infty}^{\infty}[h_s(t')+h_f(t')]|A_0(0,t-t')|^2dt'$$
$$\simeq h_s(t=0)\kappa^{-1}U_0(0,t)+h_f(\Omega=0)|A_0(0,t)|^2 \tag{42}$$

which is approximately valid over the duration of the pump pulse. The pulse energy $U_j(z,t)$ is

$$U_j(z,t)=\kappa\int_{-\infty}^{t}|A_j(z,t')|dt' \tag{43}$$

with the constant κ defined as

$$\kappa=2\varepsilon_0 nc\frac{wd}{\Gamma} \tag{44}$$

where n is the refractive index, c is the velocity of light in vacuum, ε_0 is the vacuum permittivity, and w and d are the width and heigth of the active region. For the field changes, we find

$$A_0^{(1)}(z,t)=\frac{1}{\xi_0}[e^{\xi_0 z}-1]e^{\xi_0 z/2}F_{00}(\Omega=0,t)A_0(0,t) \tag{45}$$

$$A_1^{(1)}(z,t)=\frac{1}{\xi_0}[e^{\xi_0 z}-1]e^{\xi_1 z/2}\{F_{00}(\Omega=0,t)A_1(0,t)$$
$$+F_{01}(\Omega=\Omega_1,t)A_0(0,t)\} \tag{46}$$

$$A_2^{(1)}(z,t)=\frac{1}{\bar{\xi}}[e^{\bar{\xi}z}-1]e^{\xi_2 z/2}F_{10}(\Omega=\Omega_2,t)A_0(0,t) \tag{47}$$

with the definition

$$\bar{\xi}=\xi_0+\frac{1}{2}(\xi_1-\xi_2). \tag{48}$$

The energy of the conjugate pulse at the output becomes

$$U_2^{(1)}(L,\infty)=\kappa\int_{-\infty}^{\infty}\left|A_2^{(1)}(L,t)\right|^2dt$$
$$=\frac{1}{\bar{\xi}^2}[e^{\bar{\xi}L}-1]^2e^{\xi_2 L}|h(-\Omega_1)|^2\kappa$$
$$\times\int_{-\infty}^{\infty}|A_1(0,t)|^2|A_0(0,t)|^4dt \tag{49}$$

where (17) has been used. Notice that the expression for $U_2^{(1)}$ actually is of second-order in the perturbation; this is, however, the lowest order contribution to the intensity of the conjugate signal. With heterodyne detection, the corresponding beat signal with a strong local oscillator would be of first-order in the perturbation. The integral over t in (49) depends on the pump-probe delay time τ, since $A_1(0,t)$ can be assumed to peak at $t=0$, and $A_0(0,t)$ at $t=-\tau$.

The FWM efficiency η is defined as the ratio between the output energy of the conjugate pulse and the input energy of the probe pulse

$$\eta=\frac{U_2(L,\infty)}{U_1(0,\infty)}\simeq\frac{1}{\bar{\xi}^2}[e^{\bar{\xi}L}-1]^2e^{\xi_2 L}|h(-\Omega_1)|^2$$
$$\times\frac{\int_{-\infty}^{\infty}|A_1(0,t)|^2|A_0(0,t)|^4dt}{\int_{-\infty}^{\infty}|A_1(0,t)|^2dt}. \tag{50}$$

We see that η scales with the square of the incident pump intensity [17]. Often one measures the ratio ρ of the conjugate output to the probe output

$$\rho=\frac{U_2(L,\infty)}{U_1(L,\infty)}\simeq\frac{1}{\bar{\xi}^2}[e^{\bar{\xi}L}-1]^2e^{(\xi_2-\xi_1)L}|h(-\Omega_1)|^2$$
$$\times\frac{\int_{-\infty}^{\infty}|A_1(0,t)|^2|A_0(0,t)|^4dt}{\int_{-\infty}^{\infty}|A_1(0,t)|^2dt} \tag{51}$$

where the approximation comes from neglecting terms in the expression for the probe output which are of first- and second-order in the pump power $|A_0|^2$; this is correct to second-order in the pump intensity.

Let us consider the special case of pump and probe having the same temporal dependence:

$$|A_1(0,t)|^2=r_0|A_0(0,t-\tau)|^2 \tag{52}$$

with $r_0\ll 1$ being a constant. Then

$$U_2(L,\infty)$$
$$=r_0\frac{1}{\bar{\xi}^2}\left[e^{(\xi_1-\xi_2)L/2}-e^{-\xi_0 L}\right]^2e^{(\xi_2-\xi_1)L}|h(-\Omega_1)|^2\kappa$$
$$\times\int_{-\infty}^{\infty}|A_0(L,t-\tau)|^2|A_0(L,t)|^4dt \tag{53}$$

which shows that the intensity of the conjugate scales with the third power of the pump output intensity in the low-power regime where saturation effects are negligible [15].

Let us consider also the probe output pulse energy

$$\begin{aligned}U_1(L,\infty) &= \kappa\int_{-\infty}^{\infty}\left|A_1^{(0)}(L,t)+A_1^{(1)}(L,t)\right|^2dt\\ &\simeq \kappa\int_{-\infty}^{\infty}\left|A_1^{(0)}(L,t)\right|^2dt\\ &\quad+\kappa\int_{-\infty}^{\infty}\left[A_1^{(0)*}(L,t)A_1^{(1)}(L,t)+c.c.\right]dt\\ &= e^{\xi_1 L}U_1(0,\infty)+\frac{1}{\xi_0}e^{(\xi_0+\xi_1)L/2}[e^{\xi_0 L}-1]\kappa\\ &\quad\times\int_{-\infty}^{\infty}\{F_{00}(\Omega=0,t)|A_1(0,t)|^2\\ &\quad+F_{01}(\Omega=\Omega_1,t)A_0(0,t)A_1^*(0,t)dt\}+c.c.\\ &= e^{\xi_1 L}U_1(0,\infty)+\frac{2}{\xi_0}e^{(\xi_0+\xi_1)L/2}[e^{\xi_0 L}-1]\kappa\\ &\quad\times\left\{\int_{-\infty}^{\infty}h'(t')G_\tau^{01}(t')dt'+h'(\Omega_1)G_\tau^{01}(0)\right\}.\end{aligned}\tag{54}$$

We utilized the exact expression for $F_{00}(\Omega=0,t)$ and defined the cross-correlation function

$$G_\tau^{ij}(t')=\int_{-\infty}^{\infty}|A_i(0,t-t')|^2|A_j(0,t)|^2dt\tag{55}$$

which depends implicitly on the pump–probe delay time τ. h' denotes the real part of h. The expression for $U_1(L,\infty)$ shows that the probe output contains the usual (incoherent) pump–probe signal as well as a wave mixing signal when the pump and probe overlap in time. The incoherent signal does not show any dependence on Ω_1 due to the adiabatic approximation employed in the derivation of (5).

We can also calculate the output energy of the pump pulse:

$$\begin{aligned}&U_0(L,\infty)\\ &\quad=\kappa\int_{-\infty}^{\infty}\left|A_0^{(0)}(L,t)+\Delta A_0(L,t)\right|^2dt\\ &\quad\simeq\kappa\int_{-\infty}^{\infty}\left|A_0^{(0)}(L,t)\right|^2dt\\ &\qquad+\kappa\int_{-\infty}^{\infty}\left[A_0^{(0)*}(L,t)\Delta A_0(L,t)+c.c.\right]dt\\ &\quad=e^{\xi_0 L}U_0(0,\infty)+\frac{2}{\xi_0}e^{\xi_0 L}[e^{\xi_0 L}-1]\\ &\qquad\times\kappa\int_{-\infty}^{\infty}h'(t')G_\tau^{00}(t')dt'\qquad(56)\\ &\quad\simeq e^{\xi_0 L}U_0(0,\infty)+\frac{2}{\xi_0}e^{\xi_0 L}[e^{\xi_0 L}-1]\\ &\qquad\times\int_{-\infty}^{\infty}\left[h_s'(t=0)U_0(0,t)+\kappa h_f'(\Omega=0)|A_0(0,t)|^2\right]\\ &\qquad\times|A_0(0,t)|^2dt\qquad(57)\end{aligned}$$

where the approximation (42) was used. In Appendix A, it is shown how integrals over powers of the pulse intensity can be treated. Using these results, we find

$$\begin{aligned}U_0(L,\infty)=&e^{\xi_0 L}U_0(0,\infty)\\ &\times\left\{1+\frac{e^{\xi_0 L}-1}{\xi_0}\left(h_s'(t=0)+\frac{2\eta_2}{\tau_{p0}}h_f'(\Omega=0)\right)\right.\\ &\left.\times\kappa^{-1}U_0(0,\infty)\right\}\end{aligned}\tag{58}$$

where η_2 is a constant depending on the pulse shape and τ_{p0} is the FWHM of the pump pulse intensity $|A_0(0,t)|^2$.

Equation (58) shows the relative influence of the slowly recovering carrier density saturation, through $h_s'(t=0)$, and the ultrafast saturation effects of carrier heating and SHB, through $h_f'(\Omega=0)$. Defining the critical pulsewidth $\tau_{\rm cr}$ as the pulsewidth below which the ultrafast saturation effects dominate, we find from the expressions given in Appendix A

$$\tau_{\rm cr}=2\eta_2\frac{\epsilon}{v_g g_N}.\tag{59}$$

Here, $\epsilon=\epsilon_T+\epsilon_{\rm SHB}$ is the total nonlinear gain suppression parameter and g_N is the differential gain. We considered the typical case of $\tau_1,\tau_h<\tau_{p0}<\tau_s$ and neglected the small influence of two-photon absorption. The critical pulsewidth $\tau_{\rm cr}$ can be related to the K factor which characterizes the modulation bandwidth of semiconductor lasers, $K=4\pi^2/\gamma_{\rm cav}+4\pi^2\epsilon/(g_N v_g)$, where $\gamma_{\rm cav}$ is the cavity loss rate. For large cavity loss rates, $K\simeq 4\pi^2\epsilon/(g_N v_g)$, and we have the simple relation

$$\tau_{\rm cr}=2\eta_2\frac{K}{4\pi^2}.\tag{60}$$

A typical value of K for InGaAsP semiconductor lasers is in the range of 300 to 400 ps, although it may be as large as 900 ps. [23], [24]. For $K=400$ ps, we thus get a typical critical pulsewidth of 10 ps.

The 3-dB input pulse saturation energy $U_0^{\rm sat}(0,\infty)$ is the value of $U_0(0,\infty)$ for which the pulse gain attains half its small signal value, $U_0(L,\infty)=e^{\xi_0 L}U_0(0,\infty)/2$, i.e.,

$$\begin{aligned}U_0^{\rm sat}(0,\infty)=&\frac{\kappa\xi_0}{2(e^{\xi_0 L}-1)}\\ &\times\frac{1}{(-h_s'(t=0)-2\eta_2 h_f'(\Omega=0)/\tau_{p0})}.\end{aligned}\tag{61}$$

Notice that the calculation of the 3-dB saturation energy is just at the edge of the validity of the first-order perturbative approach. However, had the characteristic saturation energy been defined at the 1-dB point, the result would have been the same as in (61) with just a different prefactor, i.e., the pulsewidth dependence is the same. In [25], we have developed an iterative technique for calculating the amplifier input-output pulse relation, which can be employed for simple and accurate numerical computation of the saturation characteristics in the case of single-pulse amplification.

In the next section, second-order perturbation theory is used to calculate the effects of pump-induced saturation on the conjugate signal.

B. Saturation Regime—Second-Order Perturbation Theory

Including the next order in the expression for the output energy of the conjugate pulse, we have

$$\begin{aligned} U_2(L,\infty) &= \kappa \int_{-\infty}^{\infty} \left|A_2^{(1)}(L,t) + A_2^{(2)}(L,t)\right|^2 dt \\ &\simeq \kappa \int_{-\infty}^{\infty} \left|A_2^{(1)}(L,t)\right|^2 dt \\ &\quad + \kappa \int_{-\infty}^{\infty} \left(A_2^{(1)*}(L,t) A_2^{(2)}(L,t) + c.c.\right) dt \\ &= U_2^{(1)}(L,\infty) + U_2^{(2)}(L,\infty). \end{aligned} \tag{62}$$

The expression for $A_2^{(2)}(L,t)$ is given by (29) with $R_2^{(1)}(z',t)$ found from (22) by insertion of the perturbation expansions for A_j:

$$\begin{aligned} R_2^{(1)}(z',t) &= \int_{-\infty}^{\infty} h(t') \left|A_0^{(0)}(z', t-t')\right|^2 A_2^{(1)}(z',t) dt' \\ &\quad + \int_{-\infty}^{\infty} h(t') A_0^{(0)*}(z', t-t') \\ &\quad \times A_2^{(1)}(z', t-t') e^{i\Omega_2 t'} A_0^{(0)}(z',t) dt' \\ &\quad + \int_{-\infty}^{\infty} h(t') A_0^{(1)}(z', t-t') \\ &\quad \times A_1^{(0)*}(z', t-t') e^{i\Omega_2 t'} A_0^{(0)}(z',t) dt' \\ &\quad + \int_{-\infty}^{\infty} h(t') A_0^{(0)}(z', t-t') \\ &\quad \times A_1^{(1)*}(z', t-t') e^{i\Omega_2 t'} A_0^{(0)}(z',t) dt' \\ &\quad + \int_{-\infty}^{\infty} h(t') A_0^{(0)}(z', t-t') \\ &\quad \times A_1^{(0)*}(z', t-t') e^{i\Omega_2 t'} A_0^{(1)}(z',t) dt'. \end{aligned} \tag{63}$$

We utilized $A_2^{(0)} = 0$ to avoid writing down all the terms. Inserting the expressions for $A_j^{(0)}$ and $A_j^{(1)}$, we get

$$\begin{aligned} A_2^{(2)}(z,t) &= \frac{1}{\xi_0 \bar{\xi}} e^{\xi_2 z/2} h(\Omega_2) A_0^2(0,t) A_1^*(0,t) \\ &\quad \times \left\{ B_1(z) \left[F_{00}(\Omega = 0, t) + h(\Omega_2) |A_0(0,t)|^2 \right] \right. \\ &\quad + B_2(z) \left[2F_{00}(\Omega = 0, t) + F_{00}^*(\Omega = 0, t) \right. \\ &\quad \left. \left. + h^*(\Omega_1) |A_0(0,t)|^2 \right] \right\} \end{aligned} \tag{64}$$

with

$$B_1(z) = \frac{\xi_0}{\xi_0 + \bar{\xi}} e^{(\xi_0 + \bar{\xi})z} - e^{\xi_0 z} + \frac{\bar{\xi}}{\xi_0 + \bar{\xi}} \tag{65}$$

$$B_2(z) = \frac{\bar{\xi}}{\xi_0 + \bar{\xi}} e^{(\xi_0 + \bar{\xi})z} - e^{\bar{\xi} z} + \frac{\xi_0}{\xi_0 + \bar{\xi}}. \tag{66}$$

We utilized an approximation similar to (40) to calculate the integrals containing $e^{i\Omega_2 t'}$. The expression (64) can be used to calculate the shape of the conjugated pulse, which in general will be different from that of the pump and probe pulses. Here, however, we shall focus on the conversion efficiency, i.e., the energy contained in the conjugated pulse.

By use of the approximation (42), the second-order contribution to the energy of the conjugate pulse becomes

$$\begin{aligned} &U_2^{(2)}(L,\infty) \\ &\quad = \frac{2}{\xi_0 \bar{\xi}^2} \kappa |h(\Omega_2)|^2 e^{\xi_2 L} [e^{\bar{\xi} L} - 1] \\ &\qquad \times \left\{ B_1(L) [h_s'(t=0) \mathcal{C}_1 + (h_f'(\Omega = 0) + h'(\Omega_2)) \mathcal{C}_2] \right. \\ &\qquad \left. + B_2(L) [3h_s'(t=0) \mathcal{C}_1 + (3h_f'(\Omega = 0) + h'(\Omega_1)) \mathcal{C}_2] \right\} \end{aligned} \tag{67}$$

with

$$\mathcal{C}_1 = \kappa^{-1} \int_{-\infty}^{\infty} |A_1(0,t)|^2 |A_0(0,t)|^4 U_0(0,t) dt \tag{68}$$

$$\mathcal{C}_2 = \int_{-\infty}^{\infty} |A_1(0,t)|^2 |A_0(0,t)|^6 dt. \tag{69}$$

These expressions can be used to investigate pulse saturation characteristics, including the effect of dispersion of the gain, for various pulse shapes and pulse overlap, as a function of detuning.

Neglecting gain dispersion ($\xi_0 = \xi_1 = \xi_2$), the expression for the conjugate pulse energy simplifies to (including both first- and second-order contributions)

$$\begin{aligned} U_2(L,\infty) &= \frac{1}{\xi_0^2} e^{\xi_0 L} [e^{\xi_0 L} - 1]^2 |h(\Omega_2)|^2 \kappa \\ &\quad \times \left\{ \mathcal{C}_0 - \frac{1}{\xi_0} (e^{\xi_0 L} - 1) [K_s \mathcal{C}_1 + K_f \mathcal{C}_2] \right\} \end{aligned} \tag{70}$$

where

$$K_f = -\mathrm{Re}\{4h_f(\Omega = 0) + h(\Omega_2) + h(\Omega_1)\} \tag{71}$$

$$K_s = -4\mathrm{Re}\{h_s(t=0)\} \tag{72}$$

$$\mathcal{C}_0 = \int_{-\infty}^{\infty} |A_1(0,t)|^2 |A_0(0,t)|^4 dt. \tag{73}$$

Assume that $|A_0(t)|^2$ and $|A_1(t)|^2$ are Gaussian pulses of the same pulsewidth, and the probe is delayed by τ with respect to the pump:

$$|A_0(t)|^2 = S(t) \tag{74}$$

$$|A_1(t)|^2 = rS(t-\tau) \tag{75}$$

$$S(t) = \exp\left(-\frac{t^2}{\tau_0^2}\right). \tag{76}$$

$\mathcal{C}_0$ and $\mathcal{C}_2$ can be evaluated exactly

$$\mathcal{C}_0 = r S_0^3 \tau_0 c_0\left(\frac{\tau}{\tau_0}\right) \tag{77}$$

$$\mathcal{C}_2 = r S_0^4 \tau_0 c_2\left(\frac{\tau}{\tau_0}\right) \tag{78}$$

with the functions c_0 and c_1 defined by

$$c_0(x) = \sqrt{\frac{\pi}{3}} \exp\left(-\frac{2x^2}{3}\right) \tag{79}$$

$$c_2(x) = \frac{\sqrt{\pi}}{2} \exp\left(-\frac{3x^2}{4}\right). \tag{80}$$

For $\mathcal{C}_1$, one can find the approximate expression (exact for $\tau = 0$):

$$\mathcal{C}_1 \approx rS_0^4\tau_0^2 c_0\left(\frac{\tau}{\tau_0}\right)\left(\frac{\sqrt{\pi}}{2}+\frac{7\tau}{24\tau_0}\right). \tag{81}$$

$\mathcal{C}_1$ has a maximum for $\tau > 0$. The τ corresponding to the maximum calculated by the approximate expression is different from the exact value by about 1%. Substituting into the expression for $U_2(L,\infty)$, one gets

$$U_2(L,\infty) \propto c_0\left(\frac{\tau}{\tau_0}\right)\left[1-A\left(\frac{\sqrt{\pi}}{2}+\frac{7\tau}{24\tau_0}\right)\right] - \frac{A}{\tau_0}\frac{K_f}{K_s}c_2\left(\frac{\tau}{\tau_0}\right) \tag{82}$$

where

$$A = \frac{1}{\xi_0}\left(e^{\xi_0 L}-1\right)K_s S_0 \tau_0. \tag{83}$$

We find that there is a value of $\tau/\tau_0 < 0$ that corresponds to a maximum for $U_2(L,\infty)$. The efficiency is maximum if the pump is delayed by an optimum value with respect to the probe, since in this case the gain is saturated less compared to the case of perfect pulse overlap. This result has been already found by Shtaif and Eisenstein in [17] for the special case of $K_f = 0$, i.e., neglecting the saturation due to the intraband effects. To give an order of magnitude estimation of the conditions under which the results of [17] are modified by the intraband dynamics, let us neglect $h(\Omega_1)$ and $h(\Omega_2)$ in the definition of K_f:

$$K_f \approx -4h_f'(\Omega = 0). \tag{84}$$

Hence

$$\frac{K_f}{K_s} \approx \frac{h_f'(\Omega=0)}{h_s'(t=0)} = \frac{\epsilon}{v_g g_N}. \tag{85}$$

As before, the term related to the fast saturation is of the same order or larger than the term related to the slow saturation if the pulsewidth is below a critical value corresponding to

$$\tau_{0,\mathrm{cr}} = \frac{\epsilon}{v_g g_N} = \frac{K}{4\pi^2}. \tag{86}$$

Let us consider now the special case where there is no time delay between the pulses, $\tau = 0$, but allow for pulse shapes other than Gaussian:

$$|A_0(0,t)|^2 = S(t); \quad |A_1(0,t)|^2 = rS(t), \quad r < 1. \tag{87}$$

Using the results of Appendix B, we then find

$$\eta = \frac{U_2(L,\infty)}{U_1(0,\infty)} = e^{\xi_0 L}|h(\Omega_2)|^2\frac{u^2}{\tau_p^2}\left\{\eta_3 - u\left[\zeta K_s + \eta_4\frac{K_f}{\tau_p}\right]\right\} \tag{88}$$

where the quantity u is related to the pump input energy $U_0(0,\infty)$:

$$u = \left(\frac{e^{\xi_0 L}-1}{\xi_0}\right)\kappa^{-1}U_0(0,\infty). \tag{89}$$

Here, η_i and ζ are constants which depend on the pulse shape (see Appendix B).

III. Results and Discussion

In the numerical examples to be presented, we have used the following set of parameter values, which are typical for an InGaAsP laser amplifier operating at wavelengths around 1.5 μm.

Basic material parameters: Effective electron mass $m_c = 0.041m_0$ (m_0 is the free-electron mass), effective hole mass $m_v = 0.46m_0$, bandgap $E_g = 0.77$ eV, refractive index $n = 3.40$, group refractive index $n_g = 3.56$, cross section for free-carrier absorption $\sigma_c = 1.0{\cdot}10^{-21}$ m^2, two-photon absorption coefficient $\beta_2 = 35$ cm/GW, "Kerr" coefficient $n_2 = -3.5{\cdot}10^{-12}$ cm^2/W, spin-orbit splitting (entering into the expression for the dipole moment d_k) $\Delta_0 = 0.33$ eV. Time constants for relaxation processes: carrier–carrier scattering time $\tau_1 = 50$ fs, dephasing time $\tau_2 = 30$ fs, temperature relaxation time (conduction band) $\tau_h = 700$ fs. Alpha-parameters: linewidth enhancement factor (associated with carrier density changes) $\alpha_N = 5$, temperature "alpha" $\alpha_T = 3$, and SHB "alpha" $\alpha_{\mathrm{SHB}} = 0$. Amplifier: cross-sectional area $A = 0.4$ $(\mu\mathrm{m})^2$, confinement factor $\Gamma = 0.3$, and "higher order" confinement factors $\Gamma_2 \simeq \Gamma, \Gamma_2' = 0.5$. Operating point: carrier density $N = 1.75{\cdot}10^{24}$ m^{-3}, $\hbar\omega_0 = 0.80$ eV (corresponding to a pump wavelength at the gain peak for this particular carrier density). These values are similar to those used in [7], [18], and [19].

From the microscopic parameter values, we calculate the following values for the differential gain and the nonlinear gain suppression parameters: $g_N = 4.1{\cdot}10^{-20}$ m^2, $\epsilon_{\mathrm{SHB}} = 3.3{\cdot}10^{-24}$ m^3, and $\epsilon_T = 8.5{\cdot}10^{-24}$ m^3. The saturation power becomes $P_{\mathrm{sat}} = \hbar\omega_0 A/(\Gamma g_N \tau_s) = 14$ mW.

Let us note that the values used for the intraband scattering times τ_2 and τ_1 are in the low end, reported values range up to 100–200 fs, and the calculated total value of the nonlinear gain suppression factor, $\epsilon = \epsilon_{\mathrm{SHB}} + \epsilon_T = 1.2{\cdot}10^{-23}$ m^3, as well as the K factor, $K = 136$ ps, are therefore also in the low end. This makes our estimate of the influence of nonlinear gain saturation on pulse amplification and four-wave mixing a conservative one, i.e., in practical cases, the role of the ultrafast dynamical processes may be even larger than in the numerical exmples presented in the next section.

A. Short-Pulse Saturation

In this section, the saturation effects under single-pulse amplification are illustrated. Based on (61), we obtain the result displayed in Fig. 1 for the pulsewidth dependence of the 3-dB input saturation energy. The regimes I–III correspond to different separations of the total response function $h(t)$ into slow h_s and fast h_f components, respectively. The appropriate choice of course depends on the actual pulsewidth; the valid pulsewidth range of each regime is indicated by solid curves in Fig. 1. Notice that there are pulsewidth ranges around each of the characteristic scattering times in which this separation cannot be made and where one has to resort to numerical calculations [21].

The dotted curve in Fig. 1 shows the constant saturation energy obtained when nonlinear gain effects (i.e., CH, SHB, and TPA) are neglected and only the influence of the carrier

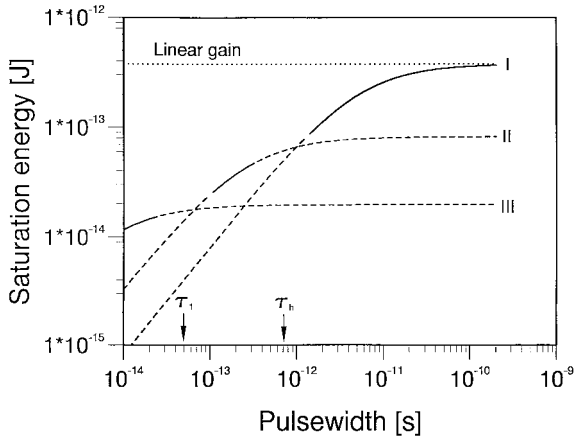

Fig. 1. Variation of 3-dB input saturation energy $U_0^{\rm sat}$ with pulsewidth τ_p. Dashed parts indicate the regions where the separation of the response function into slow and fast components compared with the relaxation times τ_h and τ_1 are not valid. The conditions for the validity of the different regimes are: I: $\tau_h < \tau_p < \tau_s$; II: $\tau_1 < \tau_p < \tau_h$; III: $\tau_p < \tau_1$.

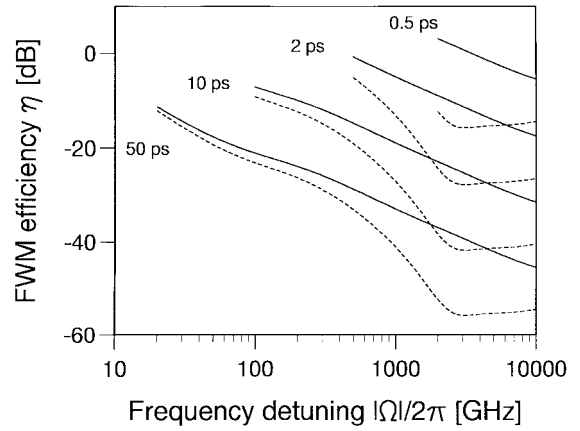

Fig. 2. Small-signal four-wave mixing efficiency η versus frequency detuning ($|\Omega|/2\pi = |\Omega_{1,2}|/2\pi$) for different pulsewidths. Solid (dashed) lines are for $\Omega_2 = \omega_2 - \omega_0 > 0$ (< 0). The input pulse energy is fixed at 100 fJ and saturation effects are neglected.

density saturation is considered. For pulses shorter than 20 ps, the error commited in neglecting nonlinear gain is 25% or larger, and for pulses shorter than 5 ps the contribution from nonlinear gain is the largest one.

B. Saturation of FWM Efficiency

Fig. 2 shows the detuning dependence of the FWM efficiency η for different widths of the pump and probe pulses. Perfect pulse-overlap has been assumed and saturation effects are neglected [i.e., $K_s = K_f = 0$ in (88)]. Solid curves correspond to $\Omega_2 = \omega_2 - \omega_0 > 0$, i.e., the conjugate is blue-shifted with respect to the pump, and dashed lines are for $\Omega_2 < 0$. The pump pulse energy at the input is kept fixed at $U_0(0,\infty) = 100$ fJ and the efficiency is only calculated for detunings significantly larger than the pulse spectral width, $|\Omega|/2\pi > 1/\tau_p$. The detuning dependence of the FWM efficiencies correspond with earlier calculations and measurements for CW beams [6]–[8].

From Fig. 2, it is clear that the FWM efficiency increases significantly as the pulses get shorter; (88) shows that η scales as $1/\tau_p^2$ for fixed pump energy in the small-signal regime, corresponding to scaling with the peak pump intensity squared [17].

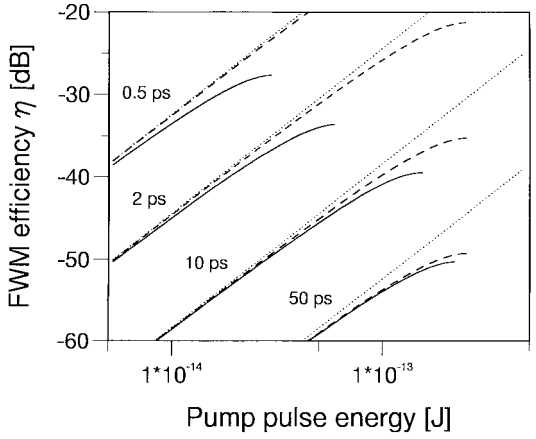

Fig. 3. FWM efficiency versus input pump pulse energy at a fixed detuning of $\Omega_2/2\pi = -2$ THz. Dotted lines: small-signal result—no saturation. Dashed lines: including only the saturation of the carrier density. Solid lines: including also saturation due to the nonlinear effects.

In Fig. 3, we investigate the saturation behavior of the FWM efficiency by plotting η versus input pump pulse energy for different pulsewidths. The FWM efficiencies were calculated at a detuning of $\Omega_2/2\pi = -2$ THz (where the absolute efficiency is less than at $\Omega_2/2\pi = +2$ THz, cf. Fig. 2), but since the detuning only influences the saturation behavior through the parameter K_f which varies little with detuning (cf. (71); $|h_f(\Omega = 0)| \gg |h(\Omega_2)|$), the result is representative for all values of the detuning.

The dotted lines in Fig. 3 are the small-signal results neglecting saturation; the dashed curves arise when only the effect of carrier density saturation (linear gain) is included, and finally the solid lines are the full result including nonlinear gain. Notice that the perturbative approach limits the validity of the results to small relative departures from the unsaturated efficiencies. Even so, it is clear that the influence of nonlinear gain becomes very large for pulses with energies in excess of only 100 fJ, when the pulsewidth is on the order of 10 ps or less. For shorter pulses, the "penalty" due to nonlinear gain rapidly increases due to the increase of peak power.

Due to the limitations of the perturbative approach, the present theory cannot be used to make any conclusions about the existence of a an optimum value of the FWM efficiency for a particular pump pulse energy. This is an important question for the practical applications of FWM and has already been discussed to some extent in the litterature. In [13], it was shown analytically that for CW beams there exists an optimum, provided that the FWM mechanisms saturate like the gain itself. In [17], the analysis was extended from the CW case and numerical calculations predicted an optimum even for pulses. However, that analysis did not inlude the saturation effects due to intraband dynamics, and from Fig. 3 we therefore conclude that the result is limited to pulses on the order of tens of picoseconds or longer. In addition, as pointed out in [13], FWM due to carrier heating by free-carrier absorption does not approach zero as the amplifier is saturated to the level

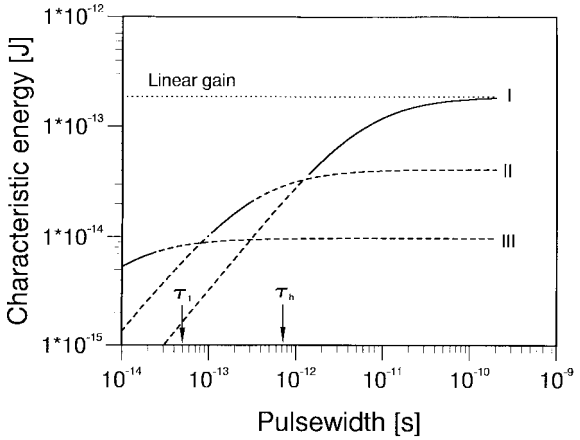

Fig. 4. Pulsewidth dependence of the characteristic energy $U_{\rm cr}$ at which the FWM efficiency is down by 3 dB from its unsaturated value. The result is—to a good approximation—independent of the detuning frequency. Curve signatures are as in Fig. 1.

of transparency, and the FWM efficiency does not exhibit a maximum in this case.

Fig. 4 depicts the pulsewidth dependence of the input pump pulse energy $U^{\rm char}$ at which the FWM efficiency is down by 3 dB from its unsaturated value. From (88):

$$U^{\rm char} = \frac{\kappa\xi_0}{2(e^{\xi_0 L}-1)}\frac{\eta_3}{\zeta K_s + \eta_4 K_f/\tau_p}. \tag{90}$$

In Fig. 4, the small detuning dependence of K_f has been neglected and the result is therefore independent of detuning. The different regimes and curve signatures correspond with Fig. 1, and since the saturation of the FWM efficiency is induced by the pump pulse saturation, the qualitative pulsewidth dependence is the same.

IV. Conclusion

Using a perturbation approach, we have derived analytical expressions for nondegenerate four-wave mixing between short optical pulses. These results should be useful for the analysis of spectroscopic measurements carried out in the linear regime with the purpose of extracting material characteristics. More importantly, the results can be used to analyze the saturation behavior of the conjugate signal, which is of practical importance, e.g., for frequency converters and demultiplexers based on FWM. As an important result, we find that ultrafast carrier dynamical processes like carrier heating and SHB have an important impact on the saturation behavior for pulses shorter than 10–20 ps. For such pulses, the ultrafast dynamics also strongly influence the optimum pump-probe overlap for the generation of the conjugate signal.

An interesting and important future application of the theory will be the analysis of the chirp characteristics of the FWM process.

Appendix A
The Material Response Function $h(t)$

The total material response function is

$$h(t) = h_N(t) + h_T(t) + h_{\rm SHB}(t) + h_{\rm TPA}(t) \tag{A1}$$

reflecting the effects of carrier depletion, carrier heating, SHB, and two-photon absorption, respectively. The real parts of h are proportional to the corresponding gain changes and the imaginary parts are proportional to the index changes. The expressions for the various terms are

$$h_N(t) = -\frac{\Gamma\varepsilon_0 ncg(\omega_0)g_N}{\hbar\omega_0}(1-i\alpha_N)[e^{-t/\tau_s}-e^{-t/\tau_1}]u(t) \tag{A2}$$

$$h_T(t) = -\frac{\Gamma\varepsilon_0 nn_g\epsilon_T g(\omega_0)}{\hbar\omega_0\tau_h}(1-i\alpha_{T_c})[e^{-t/\tau_h}-e^{-t/\tau_1}]u(t) \tag{A3}$$

$$h_{\rm SHB}(t) = -\frac{\Gamma\varepsilon_0 nn_g\epsilon_{\rm SHB}g(\omega_0)}{\hbar\omega_0\tau_1}(1-i\alpha_{\rm SHB})e^{-t/\tau_1}u(t) \tag{A4}$$

$$h_{\rm TPA}(t) = -2\varepsilon_0 cn\left(\Gamma_2'\beta_2 - i\Gamma_2\frac{4\pi}{\lambda}n_2\right)\delta(t). \tag{A5}$$

The expressions for the three first terms have been derived from semiclassical density matrix equations [19], while the last term is included phenonomenologically to account for instantaneous virtual transitions. Thus, the two-photon absorption coefficient β_2 and the "Kerr" coefficient n_2 encompass two-photon, electronic Raman and optical Stark effects [26].

In the frequency domain, we have

$$h_N(\Omega) = -\frac{\Gamma\varepsilon_0 ncg(\omega_0)g_N\tau_s}{\hbar\omega_0} \times (1-i\alpha_N)\frac{1}{(-i\Omega\tau_s+1)(-i\Omega\tau_1+1)} \tag{A6}$$

$$h_T(\Omega) = -\frac{\Gamma\varepsilon_0 nn_g\epsilon_T g(\omega_0)}{\hbar\omega_0} \times (1-i\alpha_{T_c})\frac{1}{(-i\Omega\tau_h+1)(-i\Omega\tau_1+1)} \tag{A7}$$

$$h_{\rm SHB}(\Omega) = -\frac{\Gamma\varepsilon_0 nn_g\epsilon_{\rm SHB}g(\omega_0)}{\hbar\omega_0}(1-i\alpha_{\rm SHB})\frac{1}{-i\Omega\tau_1+1} \tag{A8}$$

$$h_{\rm TPA}(\Omega) = -2\varepsilon_0 cn\left(\Gamma_2'\beta_2 - i\Gamma_2\frac{4\pi}{\lambda}n_2\right). \tag{A9}$$

Other parameters appearing in (A2)–(A9) are vacuum permittivity ε_0, speed of light in vacuum c, refractive index n, group refractive index n_g, gain $g(\omega_0)$, wavelength λ, photon energy $\hbar\omega_0$, carrier density N, differential gain $g_N = \partial g(\omega_0)/\partial N$, gain suppression factors ϵ_T and $\epsilon_{\rm SHB}$ due to carrier heating and SHB (expressions for these may be found in [19]), linewidth enhancement factors α_N, α_T, and $\alpha_{\rm SHB}$ due to the respective effects (see [19]), carrier lifetime τ_s, carrier–carrier scattering time τ_1, temperature relaxation time τ_h, Heaviside step function $u(t)$, and Dirac delta function $\delta(t)$. Finally, Γ, Γ_2, and Γ_2' are confinement factors associated with the transverse mode distribution of the waveguide, cf. [20]. For simplicity, we have neglected the transverse spatial variation of the carrier density profile in the active region, which leads to the introduction of the "higher order" confinement factor Γ_2 in the response functions h_N, h_T, and $h_{\rm SHB}$ for time scales faster than the transverse diffusion time [20].

APPENDIX B
INTEGRALS OVER POWERS OF THE PULSE INTENSITY

Let us consider the integrals

$$D_n = \int_{-\infty}^{\infty} S^n(t)dt \tag{B1}$$

where $S \propto |A|^2$ is the pulse intensity. D_1 is proportional to the pulse energy and we are interested in expressing the various integrals over the pulse in terms of the pulse energy and the pulsewidth. We shall take the pulse $S(t)$ on the form

$$S(t) = S_0 f\left(\frac{t}{\tau}\right) \tag{B2}$$

where the shape function $f(t)$ is symmetric around $t = 0$, with maximum $f(0) = 1$, and $\tau > 0$ is a parameter related to the FWHM τ_p through

$$f\left(\frac{\tau_p}{2\tau}\right) = \frac{1}{2}. \tag{B3}$$

Typical pulse shapes are $f(t) = \exp(-t^2)$, $f(t) = \mathrm{sech}^2(t)$. We find

$$D_1 = S_0 \int_{-\infty}^{\infty} f\left(\frac{t}{\tau}\right)dt = S_0 \tau N_1 \tag{B4}$$

with the definition

$$N_n = \int_{-\infty}^{\infty} f^n(t)dt. \tag{B5}$$

Also

$$D_n = S_0^n \tau \int_{-\infty}^{\infty} f^n(t)dt = S_0^n \tau N_n = \eta_n \frac{D_1^n}{\tau_p^{n-1}} \tag{B6}$$

with the constants η_n depending on pulse shape

$$\eta_n = \frac{N_n}{N_1^n}\left(\frac{\tau_p}{\tau}\right)^{n-1}. \tag{B7}$$

We also need

$$\int_{-\infty}^{\infty} S(t)U(t)dt = \frac{1}{2}D_1^2 \tag{B8}$$

where

$$U(t) = \int_{-\infty}^{t} S(t')dt' = S_0 \tau F\left(\frac{t}{\tau}\right) \tag{B9}$$

and $dF(t)/dt = f(t)$.

Finally,

$$\int_{-\infty}^{\infty} S^3(t)U(t)dt = S_0^4 \tau^2 \int_{-\infty}^{\infty} f^3(t)F(t)dt = \zeta \frac{D_1^4}{\tau_p^2} \tag{B10}$$

with

$$\zeta = \left(\frac{\tau_p}{\tau}\right)^2 \frac{1}{N_1^4} \int_{-\infty}^{\infty} f^3(t)F(t)dt. \tag{B11}$$

For square pulses, $\eta_n^{\mathrm{sq}} = 1$ and $\zeta^{\mathrm{sq}} = \frac{1}{2}$. For Gaussian pulses, $f(t) = \exp(-t^2)$:

$$\eta_n^{\mathrm{Gauss}} = \frac{1}{\sqrt{n}}\left(\frac{2\sqrt{\ln 2}}{\sqrt{\pi}}\right)^{n-1} \tag{B12}$$

$$\zeta^{\mathrm{Gauss}} = \frac{2\ln 2}{\pi\sqrt{3}}. \tag{B13}$$

The numerical values are $\eta_1^{\mathrm{Gauss}} = 1$, $\eta_2^{\mathrm{Gauss}} \simeq 0.6643$, $\eta_3^{\mathrm{Gauss}} \simeq 0.5095$, $\eta_4^{\mathrm{Gauss}} \simeq 0.4145$, and $\zeta^{\mathrm{Gauss}} \simeq 0.2548$. For secant hyperbolic pulses, $f(t) = \mathrm{sech}^2(t)$: $\eta_1^{\mathrm{sech}} = 1$, $\eta_2^{\mathrm{sech}} = \frac{2}{3}\ln(\sqrt{2}+1) \simeq 0.5876$, $\eta_3^{\mathrm{sech}} = \frac{8}{15}\ln^2(\sqrt{2}+1) \simeq 0.4143$, $\eta_4^{\mathrm{sech}} = \frac{16}{35}\ln^3(\sqrt{2}+1) \simeq 0.3130$, and $\zeta^{\mathrm{sech}} = \frac{4}{15}\ln^2(\sqrt{2}+1) \simeq 0.2072$.

REFERENCES

[1] A. D. Ellis, M. C. Tatham, D. A. O. Davies, D. Nessett, D. G. Moodie, and G. Sherlock, "40 Gbit/s transmission over 202 km of standard fiber using midspan spectral inversion," *Electron. Lett.*, vol. 31, pp. 299–301, Feb. 1995.

[2] R. Schnabel, W. Pieper, M. Ehrhardt, M. Eiselt, and H. G. Weber, "Wavelength conversion and switching of high speed data signals using semiconductor laser amplifiers," *Electron. Lett.*, vol. 29, pp. 2047–2048, Nov. 1993.

[3] M. C. Tatham, G. Sherlock, and L. D. Westbrook, "20 nm optical wavelength conversion using nondegenerate four-wave mixing," *IEEE Photon. Technol. Lett.*, vol. 5, pp. 1303–1306, Nov. 1993.

[4] S. Kawanishi and O. Kamatani, "All-optical time division multiplexing using four-wave mixing," *Electron. Lett.*, vol. 30, pp. 1697–1698, Sept. 1994.

[5] K. Kikuchi, M. Kakui, C.-E. Zah, and T.-P. Lee, "Observation of highly nondegenerate four-wave mixing in 1.5 μm traveling-wave semiconductor optical amplifiers and estimation of nonlinear gain coefficient," *IEEE J. Quantum Electron.*, vol. 28, pp. 151–156, Jan. 1992.

[6] J. Zhou, N. Park, J. W. Dawson, K. J. Vahala, M. A. Newkirk, and B. I. Miller, "Terahertz four-wave mixing spectroscopy for study of ultrafast dynamics in a semiconductor optical amplifier," *Appl. Phys. Lett.*, vol. 63, pp. 1179–1181, Aug. 1993.

[7] A. Uskov, J. Mørk, J. Mark, M. C. Tatham, and G. Sherlock, "Terahertz four-wave mixing in semiconductor optical amplifiers: Experiment and theory," *Appl. Phys. Lett.*, vol. 65, pp. 944–946, Aug. 1994.

[8] A. D'Ottavi, E. Iannone, A. Mecozzi, S. Scotti, P. Spano, R. Dall'Ara, G. Guekos, and J. Eckner, "4.3 terahertz four-wave mixing spectroscopy of InGaAsP semiconductor amplifiers," *Appl. Phys. Lett.*, vol. 65, pp. 2633–2635, Nov. 1994.

[9] G. P. Agrawal, "Population pulsations and nondegenerate four-wave mixing in semiconductor lasers and amplifiers," *J. Opt. Soc. Amer. B*, vol. 5, pp. 147–159, Jan. 1988.

[10] M. Sargent, F. Zhou, and S. W. Koch, "Multiwave mixing in semiconductor laser media," *Phys. Rev. A*, vol. 38, pp. 4673–4680, Nov. 1988.

[11] M. Yamada, "Theoretical analysis of nonlinear optical phenomena taking into account the beating vibration of the electron density in semiconductor lasers," *J. Appl. Phys.*, vol. 66, pp. 81–89, July 1989.

[12] A. Uskov, J. Mørk, and J. Mark, "Wave mixing in semiconductor laser amplifiers due to carrier heating and spectral-hole burning," *IEEE J. Quantum Electron.*, vol. 30, pp. 1769–1781, Aug. 1994.

[13] A. Mecozzi, "Analytical theory of four-wave mixing in semiconductor amplifiers," *Opt. Lett.*, vol. 19, pp. 892–894, June 1994.

[14] A. Mecozzi, S. Scotti, A. D'Ottavi, E. Iannone, and P. Spano, "Four-wave mixing in traveling-wave semiconductor amplifiers," *IEEE J. Quantum Electron.*, vol. 31, pp. 689–699, Apr. 1995.

[15] A. Mecozzi, A. D'Ottavi, F. Cara Romeo, P. Spano, R. Dall'Ara, G. Guekos, and J. Eckner, "High saturation behavior of the four-wave mixing signal in semiconductor amplifiers," *Appl. Phys. Lett.*, vol. 66, pp. 1184–1186, Mar. 1995.

[16] R. A. Fisher, Ed., *Phase Conjugate Optics*. New York: Academic, 1983.

[17] M. Shtaif and G. Eisenstein, "Analytical solution of wave mixing between short optical pulses in a semiconductor optical amplifier," *Appl. Phys. Lett.*, vol. 66, pp. 1458–1460, Mar. 1995.

[18] J. Mørk and A. Mecozzi, "Response function for gain and refractive index dynamics in active semiconductor waveguides," *Appl. Phys. Lett.*, vol. 65, pp. 1736–1738, Oct. 1994.
[19] _____, "Theory of the ultrafast optical response of active semiconductor waveguides," *J. Opt. Soc. Amer. B*, vol. 13, pp. 1803–1816, Aug. 1996.
[20] A. Mecozzi and J. Mørk, "Theory of heterodyne pump-probe experiments with femtosecond pulses," *J. Opt. Soc. Amer. B*, vol. 13, pp. 2437–2452, Nov. 1996.
[21] A. Uskov, J. Mørk, and J. Mark, "Theory of short-pulse gain saturation in semiconductor laser amplifiers," *IEEE Photon. Technol. Lett.*, vol. 4, pp. 443–446, 1992.
[22] K. L. Hall, G. Lenz, and E. P. Ippen, "Femtosecond time domain measurements of group velocity dispersion in diode lasers at 1.5 μm," *J. Lightwave Technol.*, vol. 10, pp. 616–619, May 1992.
[23] K. Uomi, T. Tsuchiya, M. Aoki, and N. Chinone, "Oscillation wavelength and laser structure dependence of nonlinear damping effect in semiconductor lasers," *Appl. Phys. Lett.*, vol. 58, pp. 675–677, Feb. 1991.
[24] J. Shimizu, H. Yamada, S. Murata, A. Tomita, M. Kitamura, and A. Suzuki, "Optical-confinement-factor dependence of the K factor, differential gain, and nonlinear gain coefficient for 1.55 μm InGaAs/InGaAsP MQW and strained MQW lasers," *IEEE Photon. Technol. Lett.*, vol. 3, pp. 773–776, Sept. 1991.
[25] A. Mecozzi and J. Mørk, "Saturation induced by picosecond pulses in semiconductor optical amplifiers," *J. Opt. Soc. Amer. B*, vol. 14, March 1997.
[26] M. Sheik-Bahae and E. W. Van Stryland, "Ultrafast nonlinearities in semiconductor laser amplifiers," *Phys. Rev. B*, vol. 50, pp. 14171–14178, Nov. 1994.

J. Mørk, photograph and biography not available at the time of publication.

A. Mecozzi, photograph and biography not available at the time of publication.